Neuron, Vol. 47, 827–839, September 21, 2005 ©2005 Elsevier Inc. DOI 10.1016/j.neuron.2005.07.009

Subplate Neurons Regulate Maturation of Cortical Inhibition and Outcome of Ocular Dominance Plasticity

Patrick O. Kanold[1] and Carla J. Shatz[1,*]
[1] Department of Neurobiology
Harvard Medical School
Boston, Massachusetts 02115

Summary

Synaptic plasticity during critical periods of development requires intact inhibitory circuitry. We report that subplate neurons are needed both for maturation of inhibition and for the proper sign of ocular dominance (OD) plasticity. Removal of subplate neurons prevents the developmental upregulation of genes involved in mature, fast GABAergic transmission in cortical layer 4, including GABA receptor subunits and KCC2, and thus prevents the switch to a hyperpolarizing effect of GABA. To understand the implications of these changes, a realistic circuit model was formulated. Simulations predicted that without subplate neurons, monocular deprivation (MD) paradoxically favors LGN axons representing the deprived (less active) eye, exactly what was then observed experimentally. Simulations also account for published results showing that OD plasticity requires mature inhibition. Thus, subplate neurons regulate molecular machinery required to establish an adult balance of excitation and inhibition in layer 4, and thereby influence the outcome of OD plasticity.

Introduction

Experience-dependent plasticity during the "critical period" has been studied by examining ocular dominance (OD) columns in visual cortex of higher mammals. During the critical period of development, sensory experience shapes cortical circuitry, as seen by the effects of monocular deprivation (MD) in the mammalian visual cortex. MD shifts the balance of thalamic inputs representing the two eyes within cortical layer 4: OD columns representing the deprived eye (DE) are smaller, while those representing the nondeprived eye (NDE) are larger than normal. This change in the pattern of geniculocortical projection to layer 4 is an anatomical manifestation of the physiologically assessed "ocular dominance shift," which represents the strengthening of the more active (NDE) inputs and weakening of the less active (DE) inputs (Hubel et al., 1977; Wiesel and Hubel, 1963).

Maturation of inhibitory cortical circuits is thought to be key in regulating the critical period (Hensch, 2004). Mice lacking an isoform of the GABA synthesizing enzyme GAD65, which are thus deficient in fast GABAergic inhibition, lack OD plasticity; this defect can be rescued by augmenting GABAergic inhibition pharmacologically (Hensch et al., 1998). In mice overexpressing BDNF, the GABAergic circuit matures early, accompanied by an early opening and closing of the critical period (Hanover et al., 1999; Huang et al., 1999). The critical period can also be triggered precociously by pharmacologically enhancing GABAergic transmission (Fagiolini and Hensch, 2000). However, the intrinsic cells and circuits within cortex that normally drive this maturation have not been extensively studied.

Subplate neurons could be crucial players in this process. During prenatal and early postnatal development, subplate neurons provide the dominant excitatory input to the developing cortex (Friauf et al., 1990; Friauf and Shatz, 1991; Herrmann et al., 1994). They are the first cortical neurons to receive functional thalamic input, and subplate axons relay activity from thalamus to layer 4 even before thalamic axons themselves grow into layer 4 (Friauf et al., 1990; Friauf and Shatz, 1991; Herrmann et al., 1994) (Figure 1A). This early circuit is required for initial strengthening of thalamocortical synapses and subsequent formation of cortical columns (Kanold et al., 2003). Subplate neurons are present during the period of GABAergic maturation and the critical period, during which time they are gradually eliminated by programmed cell death (Allendoerfer and Shatz, 1994), leaving in place the adult circuit in which thalamic axons directly synapse upon layer 4 neurons (Figure 1A). To examine if subplate neurons are needed for maturation of inhibition, they were ablated selectively by means of p75-immunotoxin or kainic acid injection (Ghosh et al., 1990; Kanold et al., 2003) well before their normal period of death and before maturation of GABAergic circuits (Chen et al., 2001; Golshani et al., 1997; Huntsman et al., 1999). Here we show that in the absence of the subplate, GABAergic synaptic transmission fails to mature and this failure is associated with a change in the way that monocular visual deprivation affects thalamocortical synaptic connectivity representing the deprived and nondeprived eyes in layer 4.

Results

When subplate neurons are removed between P6-P9 in cat by means of localized injections of p75-immunotoxin or kainic acid into the subplate, as shown previously, the ablation is highly selective for subplate neurons and spares neurons of cortical plate (Ghosh and Shatz, 1992; Kanold et al., 2003; Lein et al., 1999; Experimental Procedures) (Figure 1B; see also Figure S1 in the Supplemental Data). The state of inhibitory circuits was assessed ~3–4 weeks post ablation.

Maturation of GABAergic Synaptic Transmission Requires Subplate Neurons

To determine if GABAergic circuitry is altered following subplate neuron ablation, we first examined the expression of genes required for adult fast inhibitory synaptic transmission. $GABA_A$ receptors are assembled from multiple subunits whose exact composition is regulated developmentally in cat (Figure 1C). Mature cortical $GABA_A$ receptors contain $\alpha 1$ and $\gamma 2$ subunits, whereas $\alpha 2$ and $\alpha 3$ are prominent at early ages (Chen et al., 2001; Golshani et al., 1997; Huntsman et al., 1999). Following

*Correspondence: carla_shatz@hms.harvard.edu

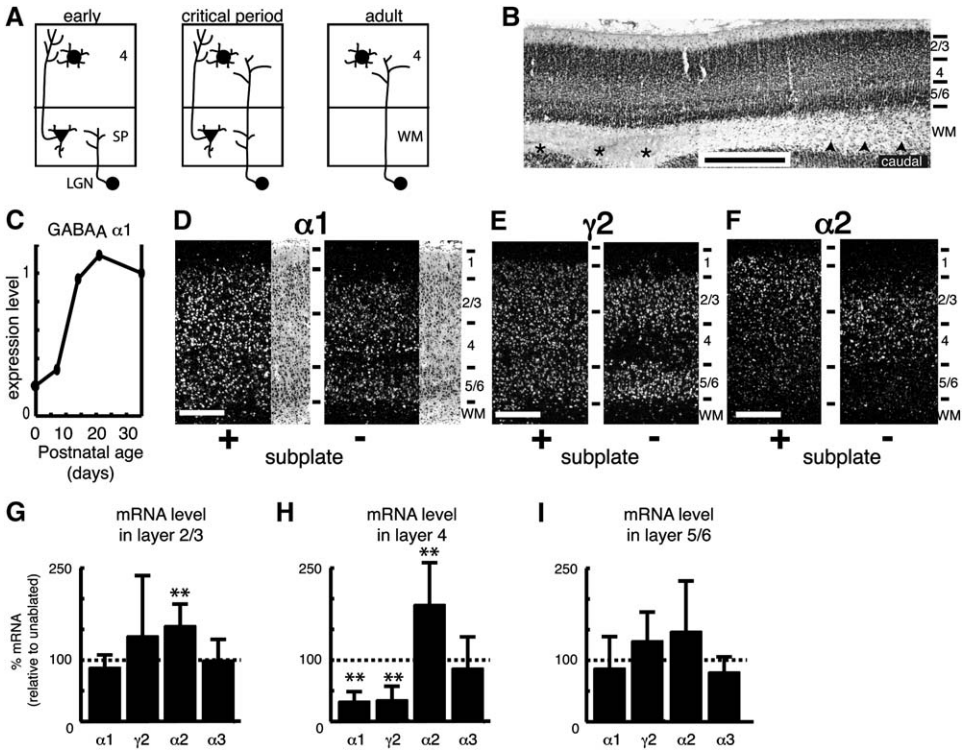

Figure 1. Subplate Ablation Prevents Developmental Switch in $GABA_A$ Receptor Subunit Expression

(A) Schematic of subplate circuits in cat visual cortex (Allendoerfer and Shatz, 1994). Early: Subplate neurons receive inputs from LGN neurons and subplate axons project to cortical layer 4. Onset of critical period (coincides with time of subplate ablation): Both subplate neurons and LGN neurons project to layer 4. Adult: Subplate neurons have been eliminated by programmed cell death and layer 4 cells receive inputs from LGN axons.

(B) Immunohistochemistry for NeuN (neuron-specific marker) confirms selective loss of subplate neurons (asterisks) at p75-immunotoxin injection sites. Note abundant subplate neurons (arrowheads) in white matter distant from injection sites (Kanold et al., 2003; Experimental Procedures). Scale bar, 1 mm.

(C) Quantitative PCR for $GABA_A$ receptor α1 subunit mRNA expression in cat visual cortex at P0, P7, P14, P21, and P35 (n = 1 animal per time point). Graph shows the relative expression levels of α1 (normalized to level at P35) at different ages. Note rapid increase of α1 mRNA in second postnatal week.

(D–F) Darkfield autoradiographs of in situ hybridizations for $GABA_A$ receptor subunit α1 (D), γ2 (E) and α2 (F) mRNA (adjacent sections) at P26 following subplate ablation at P5. Scale bar, 0.5 mm.

(G–I) Quantification of $GABA_A$ receptor subunit mRNA levels (mean + SD) in layers 2/3, 4, and 5/6 after subplate ablation using densitometric measurements (n = 5–8 sections for each subunit, n = 4–5 animals each; see Experimental Procedures). Asterisks indicate significant differences between ablated and control (**$p < 0.05$).

subplate ablation, the expression of α1 and γ2 subunits of the $GABA_A$ receptor is lower in layer 4 of subplate-ablated cortex than in neighboring unablated regions (33% ± 16% and 35% ± 22%, respectively, both $p < 0.001$, Student's t test, n = 5 animals) (Figures 1D, 1E, and 1H). In contrast, expression of those subunits in layers 2/3 and 5/6 within ablated regions is close to, if not completely, normal (2/3: 88% ± 21% and 139% ± 98%; 5/6: 87% ± 52% and 131% ± 47%, Student's t test, all $p > 0.1$, n = 5 animals) (Figures 1G and 1I). Moreover, levels of $GABA_A$ receptor mRNA for the "immature" α2 subunit are higher in layer 4 within subplate-ablated cortex than in unablated regions (191% ± 68%, Student's t test, $p < 0.025$, n = 4 animals) (Figures 1F–1I). The increased in situ signal for α2 in layer 4 also confirms that layer 4 neurons are abundant. Thus, without subplate neurons, $GABA_A$ receptor maturation in layer 4, the major target of both subplate and LGN axons, does not occur, whereas it occurs essentially normally in the other cortical layers.

The lack of $GABA_A$ receptor subunit α1 and abundance of α2 after subplate ablation is reminiscent of earlier developmental stages (Chen et al., 2001; Golshani et al., 1997; Huntsman et al., 1999) (Figure 1C). This fact suggests that other aspects of GABAergic maturation might not proceed normally without subplate neurons. Early in development, GABA is depolarizing and a key step in GABAergic maturation is the switch to a hyperpolarizing effect of GABA (Owens et al., 1996; Rivera et al., 1999). In many, if not all, neurons, the hyperpolarizing effect of GABA requires expression of a K^+-Cl^--cotransporter KCC2, which lowers intracellular chloride concentration (Hubner et al., 2001; Rivera et al., 1999) and thus the sign of fast GABAergic input mediated by $GABA_A$ receptors. In rodents, KCC2 is upregulated postnatally (Ganguly et al., 2001; Hubner et al., 2001; Lu et al., 1999; Owens et al., 1996; Rivera et al., 1999), and this postnatal increase also occurs in cat, to reach high uniform levels by P35 (Figure 2A). These in situ hybridization data were confirmed by quantitative PCR, showing the high KCC2 expression attained by P35 (Figure 2B).

This developmental upregulation of KCC2 mRNA, however, fails to occur in subplate-ablated cortex. In

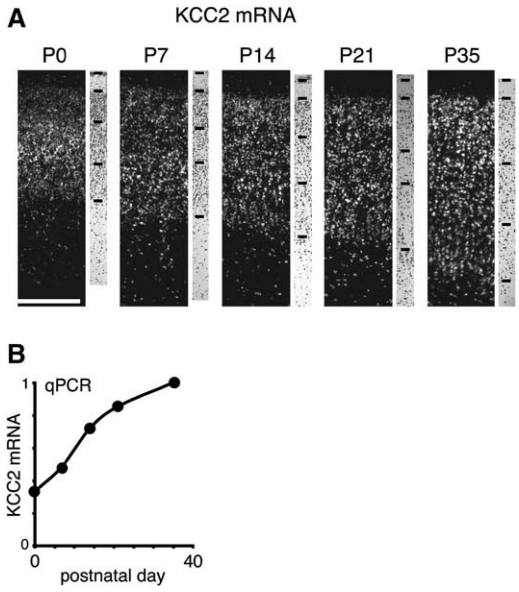

Figure 2. Maturation of KCC2 Expression in Cat Visual Cortex

(A) Darkfield autoradiographs of in situ hybridizations of KCC2 performed on horizontal sections (P0, P7, P14, P21, and P35). Adjacent cresyl violet stains delineate cortical layers. Scale bar, 0.5 mm.

(B) Developmental increase in KCC2 mRNA expression in cat visual cortex measured with quantitative PCR (n = 1 animal per time point). Expression levels of KCC2 at each age are normalized to P35 level. Note significant increase in KCC2 mRNA by second postnatal week.

situ hybridizations reveal that within layer 4, mRNA levels are vastly lower than in unablated regions, whereas expression in other cortical layers is close to normal (Figures 3A–3D). Instead of being similar to levels in layer 2/3 (Figures 3A and 3D), KCC2 mRNA levels in layer 4 at P26 after subplate ablation at P5 are 33% ± 25% of that of unmanipulated layer 4 (Figures 3B and 3C), a level similar to that normally present at the age of ablation (~P5–P7, Figure 2B). Areas of low KCC2 expression in layer 4 also have abnormally high expression levels of BDNF in layer 4 and layers 2/3 (Figure 3D). The low KCC2 levels do not reflect a developmental delay in upregulation, but rather represent a permanent block in upregulation, since KCC2 levels in ablated areas are low even at >P50 (n = 3 animals, Figure 3E). Nor are the low levels of KCC2 due to the loss of layer 4 neurons, which are still present in abundance (Figure 3: cresyl violet images shown adjacent to in situ hybridizations; Figure 3D BDNF signal; also Figure 1; Figure S1). In addition, layer 4 neurons, as shown below, can be recorded using whole-cell or calcium imaging methods. This block in KCC2 upregulation occurs only if injections of p75-immunotoxin or kainic acid are made directly into the subplate, since injections located within layer 4, or sham (saline) injections into the subplate, do not have similar effects on KCC2 expression (Figures 3F and 3G) or on OD column formation (Ghosh and Shatz, 1992; Kanold et al., 2003). These observations indicate that subplate ablation selectively prevents the normal developmental upregulation of KCC2 mRNA in layer 4 neurons, but not in other cortical layers.

The developmental upregulation of KCC2 and $GABA_A$-α1 is also prevented by chronic blockade of glutamatergic synaptic transmission with minipump infusion of NBQX plus AP5 between P6–P20 (Figure 3H). This experiment complements those in which subplate neurons are ablated, and taken together, the results show that glutamatergic inputs to cortical neurons (including those from subplate neurons) are required for GABAergic maturation.

Subplate neurons, by controlling $GABA_A$ receptor subunit maturation in layer 4, might act as crucial in vivo cellular players for driving maturation of functional inhibitory circuitry. If so, then there should be associated physiological changes in postsynaptic response properties at fast GABAergic synapses. We first investigated the magnitude of GABAergic responses by whole-cell patch-clamp recordings (which alter the intracellular chloride concentration) from layer 4 neurons in slices from ablated or unablated cortex. These recordings revealed that bath application of muscimol (a $GABA_A$ agonist) evokes currents that are 85% smaller in neurons in layer 4 of ablated regions than in neurons located in nearby unmanipulated regions (Figure 4A), consistent with lower expression of mature $GABA_A$ receptor mRNAs.

To assess the functional characteristics of GABA action, muscimol-evoked currents were recorded in layer 2/3 or layer 4 neurons in slices from ablated (see Figure 4D) or unablated hemispheres using gramicidin perforated patch recordings so as not to disturb the intracellular chloride concentration. Muscimol application to layer 4 cells in the ablated zone generated inward (depolarizing) current (Figures 4B and 4E), which reversed upon patch rupture and washout of intracellular chloride. In contrast, muscimol evoked outward currents in cells located in all layers of unablated hemispheres and also in layer 2/3 neurons situated just above the ablation site (Figures 4C and 4E). These currents increased in amplitude after patch rupture into whole cell mode (Figure 4C, right). In contrast to their abnormal functional properties, layer 4 neurons showed no obvious morphological abnormalities (Figure 4D).

Because inward currents are depolarizing, it was possible to confirm these observations by measuring intracellular Ca^{2+} levels using Fura 2-AM. In slices from subplate-ablated hemispheres, bath application of muscimol increases intracellular Ca^{2+} in layer 4 neurons (Figure 4F), consistent with depolarization. In contrast, there was no detectable fluorescence increase (but possibly even a slight decrease) in layer 4 of unablated hemispheres (Figure 4F). These results were confirmed by pressure application of muscimol from a pipette (Figure 4G). The muscimol-evoked Ca^{2+} fluorescence could be blocked by application of picrotoxin, a selective $GABA_A$ antagonist (Figure 4G). Together, these experiments show that GABA action remains depolarizing in layer 4 in the absence of subplate neurons. Moreover, the effect is selective for layer 4, since neurons in layers 2/3 acquire normal hyperpolarizing responses to GABA application. Prior in vivo microelectrode and in vitro whole-cell slice recordings indicated that spontaneous neural activity in cortex is increased after subplate neuron ablation (Kanold et al., 2003); the observation that inhibition remains depolarizing can explain this increased spontaneous activity. Taken together with the in situ hybridization data above, these results indicate that subplate neurons are needed to trigger the normal developmental switch in GABAergic synaptic transmission

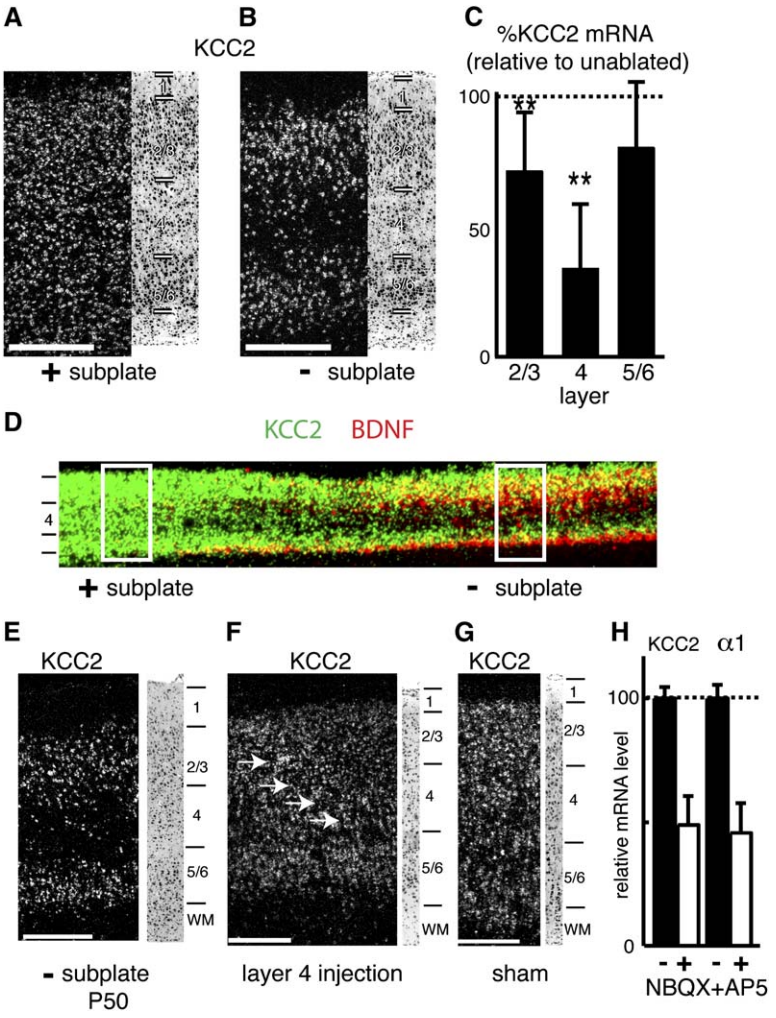

Figure 3. Subplate Neuron Ablation Prevents Developmental Upregulation of KCC2 mRNA in Layer 4 of Visual Cortex

(A and B) Darkfield autoradiographs of in situ hybridizations for KCC2 mRNA in P26 visual cortex (subplate ablation at P5). Within ablated zones KCC2 mRNA expression is decreased, particularly within cortical layer 4. Cresyl violet stain (right) indicates normal histology. Scale bar, 0.5 mm.

(C) Densitometric measurements of KCC2 mRNA levels (mean + SD) after subplate ablation (n = 10 sections from n = 6 animals; see Experimental Procedures). KCC2 levels in layer 4 are reduced to 33% ± 25% compared to layer 4 in unablated regions (**$p < 0.005$); KCC2 levels in other layers are close to unablated regions (layer 2/3: 70% ± 19%, $p < 0.05$; layers 5/6: 80% ± 25%, $p > 0.1$).

(D) Superposition of BDNF with KCC2 mRNA expression patterns shows that in ablated regions, KCC2 (green) expression is decreased in areas of increased BDNF (red) expression (right box). KCC2 levels are high in layer 4 of unablated areas (left box) coincident with low BDNF levels. Layer 4 cells are abundant in layer 4 of ablated areas (right box) and express high levels of BDNF, but low levels of KCC2, as indicated by the lack of yellow label. Note the abundance of yellow label in layer 2/3 of ablated areas, indicating high BDNF and KCC2 expression.

(E) In situ hybridizations for KCC2 mRNA at P50 following subplate ablation at P5. Note persistence of low levels of KCC2 mRNA in layer 4 (n = 3 animals). Scale bar, 0.5 mm.

(F and G) In situ hybridizations for KCC2 mRNA following direct injection of kainate into layer 4 (at P5, n = 3 animals) ([F], arrows indicate needle track) or injection of saline into subplate (at P7, n = 1 animal) (G) show normal levels of KCC2 mRNA expression in layer 4, consistent with previous control experiments (Ghosh and Shatz, 1992; Lein et al., 1999). Cresyl violet stain (right) indicates normal histology. Scale bars, 0.5mm.

(H) Relative mRNA levels of KCC2 and $GABA_A$-α1 in visual cortex infused between P6–P20 (n = 4 animals) with NBQX plus AP5 (+) and unmanipulated cortex (−) (see Experimental Procedures) (mean + SD). Levels of KCC2 and $GABA_A$-α1 were reduced after infusion compared to control (KCC2: 47% ± 28%; $GABA_A$-α1: 48% ± 29%; both $p < 0.01$; n = 11 sections each from infused and control hemisphere). Relative mRNA levels of KCC2 and $GABA_A$-α1 were unchanged in saline-infused brains (KCC2: 109% ± 32%; $GABA_A$-α1: 120% ± 30%; both $p > 0.1$; n = 8 sections each from infused and control hemisphere; n = 2 animals).

from an immature, depolarizing state to a mature hyperpolarizing state within cortical layer 4.

A Computational Model of the Subplate Circuit Predicts Altered Layer 4 OD Plasticity

Intact GABAergic inhibition is thought to be required for OD plasticity, implying that subplate neuron ablation might also alter plasticity in layer 4 since (1) it alters maturation of cortical inhibition and (2) subplate neurons are present during the critical period. To gain an initial understanding of how OD plasticity might be modulated by the strength of inhibition and the subplate-to-layer 4 circuit, a computational model was formulated (see Experimental Procedures). The model is based on minimal assumptions and on the known state of the circuit at the beginning of the critical period, when layer 4 neurons initially receive synaptic inputs from both subplate neurons and LGN neurons (Figure 5A) (Friauf et al., 1990; Friauf and Shatz, 1991; Hubel et al., 1977; Shatz and Stryker, 1978). At this time, synapses are assumed to undergo long-term changes according to asymmetric spike-time dependent plasticity (STDP) rules, which strengthen synaptic inputs to layer 4 neurons that are capable of initiating an action potential and weaken those that are not (Figure 5A, inset). This assumption is reasonable and is based upon studies of synaptic plasticity in the visual system of many species at many ages (Abbott and Nelson, 2000; Bi and Poo, 2001; Dan and Poo, 2004; Froemke and Dan, 2002; Song et al., 2000; Yao and Dan, 2001), but to date no comparable experiments have been performed in cat layer 4 during the critical period. Simulations were started at an initial state in which the strength of thalamocortical synaptic inputs (as measured by EPSC amplitude) from LGN neurons of both eyes to a layer 4 neuron are equal but smaller than those from subplate neurons, consistent with physiological measurements (Friauf et al., 1990; Friauf and Shatz, 1991).

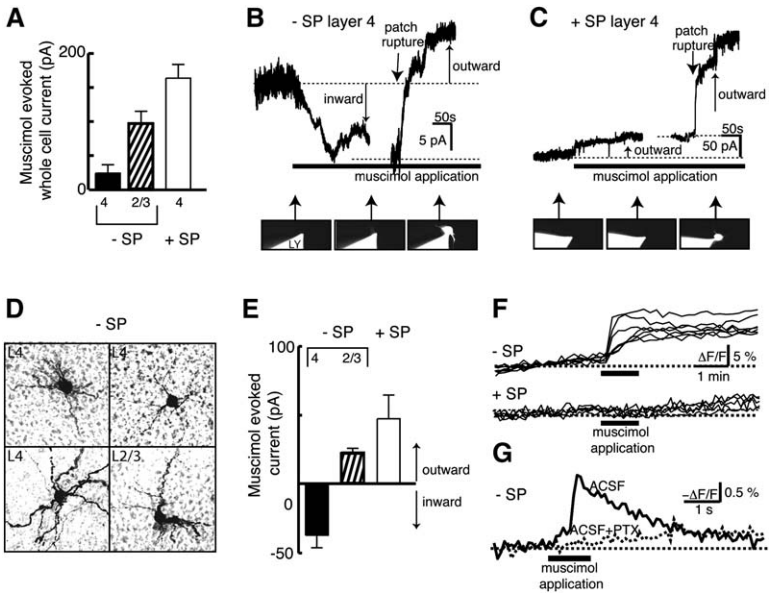

Figure 4. GABA Is Depolarizing in Subplate-Ablated Cortex

(A) Summary histograms (mean + SD) of muscimol-evoked currents in whole-cell patch recordings from cells in layer 4 of ablated regions and in unmanipulated hemispheres. Muscimol-evoked currents were smaller in layer 4 neurons within subplate-ablated zones (24.1 ± 34.9 pA, n = 8 cells) than in layer 4 neurons of unmanipulated regions (164.7 ± 49.2 pA, n = 6 cells, $p < 0.01$).

(B and C) $GABA_A$ receptor activation by bath application of muscimol (50–100 μM) generates inward currents in layer 4 neurons in slices from subplate-ablated cortex as detected by gramicidin perforated patch recordings at P27–P35 (n = 42 cells in four animals ablated at P7). Cells were held at ~ −60 mV, and the pipette contained a low Cl^- solution ($E_{Cl} \sim -78$ mV); thus, $GABA_A$ activation leads to outward currents in whole-cell mode. (B) Trace shows membrane current during muscimol application (horizontal bar), which evokes inward current; current reverses upon patch rupture into whole-cell mode (right trace). Patch integrity was monitored by including Lucifer yellow (LY) in the pipette; left two images show LY fluorescence in recording pipette before and during muscimol application. Right image shows pipette and filled cell after patch rupture. (C) Muscimol evokes outward currents in a layer 4 neuron from unmanipulated hemisphere; current increased upon patch rupture (right trace). Note larger current amplitude after patch rupture in layer 4 cells from unablated zones than in cells from ablated zones (see panel [A]).

(D) LY-filled cells in cortex of subplate-ablated zone have normal morphology. LY was detected after recording and tissue processing by biotinylated anti-LY antibody. L4 = layer 4; L2/3 = layer 2/3.

(E) Summary histograms (mean + SD) of muscimol-evoked currents in perforated patch recordings from cells in ablated regions (layer 4: n = 13; layer 2/3: n = 12) and in unmanipulated hemispheres (layer 4: n = 12).

(F and G) Bath (50–100 μM) or pressure application (250 μM) of muscimol (horizontal bars) generates Ca^{2+} influx in layer 4 cells from subplate-ablated cortex (n = 4 animals, ablated at P8–P9; imaged at P27–P42) as detected by Ca^{2+} imaging. (F) Mean fluorescence signal (dF/F, 340/380 nm) recorded from cells in ablated (n = 7 cells, upper traces) or unablated (n = 5 cells, lower traces) regions. Bath application of muscimol increases fluorescence in 98/106 cells in ablated zones (n = 10 slices from n = 2 animals), but does not increase fluorescence in unablated regions (n = 72/76 cells, n = 5 slices from n = 2 animals). (G) Pressure application of muscimol increases fluorescence (−dF/F at 380 nm, ten repetitions averaged) in neurons from ablated zones in standard ACSF (n = 32 cells in ten slices from n = 2 animals). Increases are blocked by 0.1 mM picrotoxin (ACSF + PTX, n = 13 cells in six slices from n = 2 animals). Muscimol application in unmanipulated regions does not increase Ca^{2+} fluorescence (n = 13 cells, not shown).

Because subplate neurons are present before and during the critical period, we first examined whether OD *plasticity*—that is, the ability of thalamocortical connections in layer 4 serving the two eyes to change their strength in response to MD—is recapitulated correctly in the model circuit including subplate neurons. To investigate the effect of MD, the NDE LGN neuron firing rate was set higher than the DE firing rate (Miller et al., 1989b). When subplate neurons are present, EPSCs driven by the NDE in layer 4 neurons are strengthened over time, while DE and subplate EPSCs weaken (Figure 5B) such that the more active NDE ultimately accounts for over 80% of the total LGN input to layer 4, resulting in the experimentally observed OD shift toward the NDE.

In fact, a bias in favor of the contralateral eye is observed experimentally in the response of layer 4 cells to visual stimulation at early ages, with larger contralateral biases observed in layers 2/3 (Albus and Wolf, 1984; Hubel and Wiesel, 1963; LeVay et al., 1978). Simulations performed with an initial bias toward one eye showed that the NDE can overcome biases toward the DE in the observed physiological range (Figure 5C), whereas large initial biases outside the physiological range prevent the NDE from strengthening, likely because the NDE is too weak at the outset (Figure 5C).

Intact GABAergic inhibition suppresses spontaneous firing and consequently decreases the frequency of EPSCs in cortical neurons (Baumfalk and Albus, 1987). To investigate the effects of weak or absent intracortical GABA inhibition on the intact developing thalamocortical circuit, the frequency of spontaneous EPSCs ($\lambda_{intraspont}$) was increased, and the OD shift in layer 4 after MD quantified by computing an OD bias index (Figure 5D). Simulations show that when spontaneous EPSCs onto layer 4 neurons are low (i.e., at high levels of inhibition), MD generates a shift in OD toward the nondeprived eye (bias index >0), as expected. However, as the rate of spontaneous EPSCs impinging on layer 4 neurons increases (i.e., as inhibition decreases), the OD bias decreases to a value of 0, where MD does not produce an OD shift at all (Figure 5D). Note that in the face of a significant increase in EPSC rates sufficient to prevent OD plasticity, there is only a modest increase in the *spiking* rate of layer 4 neurons (Figure 5D, lower panel). As spontaneous EPSC rates increase even further, a paradoxical OD shift (bias index <0) toward the DE is predicted. Such paradoxical OD shifts have in fact been observed (see Discussion).

To examine the usefulness of the model further, the effects of MD plus subplate ablation were simulated.

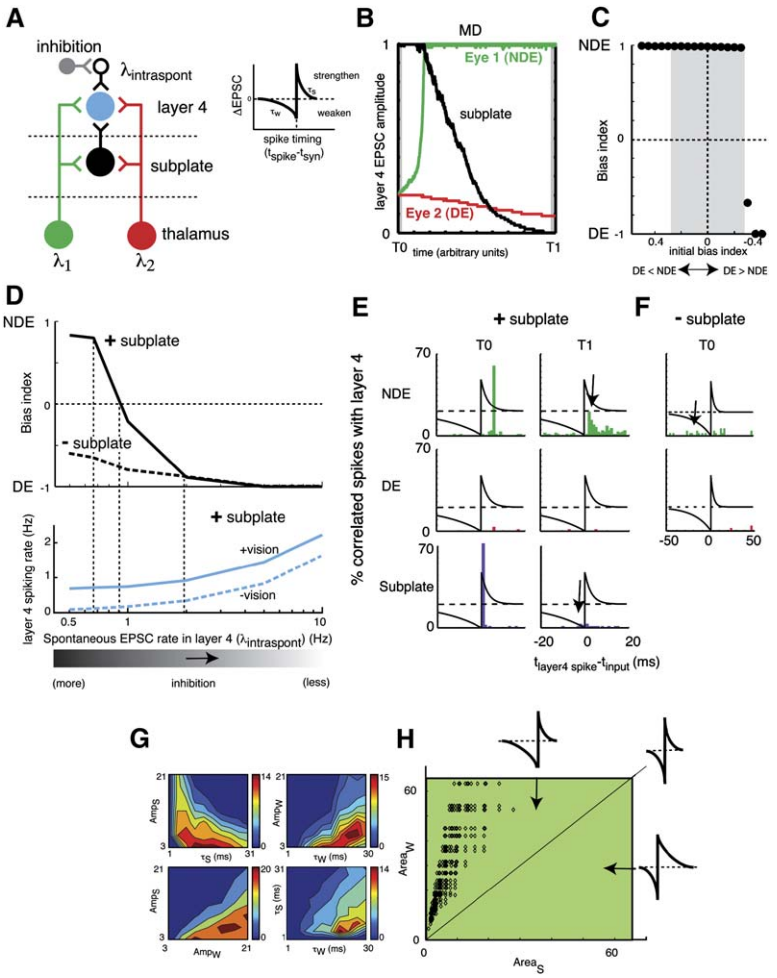

Figure 5. Subplate Neurons Control Sign of OD Plasticity in Simulations

(A) Model schematic of LGN-subplate-cortex circuit. Layer 4 (blue) and subplate neurons (black) each receive input from two LGN axons (one from each eye: green, red). Layer 4 neuron receives inputs from subplate neuron and spontaneous inputs from local cortical circuits (Douglas and Martin, 2004). Frequency of thalamic inputs $\lambda_{1,2}$ = 5 Hz and frequency of spontaneous intracortical EPSC inputs $\lambda_{intraspont}$ = 0.5 Hz. (Inset) STDP learning rule with window for strengthening or weakening.

(B) Developmental changes in EPSC amplitude in layer 4 neurons after MD (decrease in λ of the DE from 5 Hz to 0.3 Hz). Initially, layer 4 inputs are dominated by subplate while thalamic inputs (red, green) are weak. Over time, NDE LGN input (green) strengthens, while DE (red) inputs weaken.

(C) Relation between OD bias = (NDE − DE)/(NDE + DE) at the end of the simulations when the simulations were started with a developmental bias toward the DE or NDE. An OD bias of ~1 is the expected outcome following MD under normal circumstances and predicts a shift in favor of the NDE. Bias toward the DE results in normal OD plasticity toward the NDE if biases are within the physiological range (gray box). Initial biases toward the NDE always result in normal OD plasticity toward the NDE.

(D) Relation between OD bias and spontaneous EPSC rate in layer 4 ($\lambda_{intraspont}$; inversely related to amount of tonic inhibition) (upper panel). At low spontaneous EPSC rates the OD bias is ~1. For certain intermediate rates (~1 Hz), neither strengthening nor weakening is predicted (OD bias = 0), indicating that OD plasticity is absent. If spontaneous EPSC rates increase further, the NDE weakens to levels below that of the DE; paradoxical plasticity (OD bias < 0) results. Without subplate, paradoxical plasticity is predicted at all spontaneous EPSC rates (dashed line). Lower panel shows spontaneous (dashed blue line) and visually driven (solid blue line) spiking rates of the layer 4 neuron resulting from variations in spontaneous EPSC rate ($\lambda_{intraspont}$).

(E) Simulated correlations between layer 4 neuron firing and its respective inputs (DE, NDE, subplate) plotted at two different time points (T0, T1; gray lines in [B]). Learning rule is superimposed to identify events causing synaptic strengthening or weakening. At T0, note short latency correlation between subplate and layer 4 spikes; there is also a long latency correlation between NDE and layer 4 firing, due to disynaptic connectivity. With time, short latency correlations between NDE and layer 4 spikes emerge (T1: arrow), and correlations from DE disappear.

(F) Without subplate neurons, correlations in activity between NDE and layer 4 are absent and many spikes fall into the weakening window (arrow), predicting experimentally observed paradoxical plasticity.

(G) Analysis of the 384 parameter sets that replicated the experimental data. Plotted are relations between pairs of parameters. Amp = Amplitude of ΔEPSC (in 10^−3). The colors indicate the number of parameter sets with the particular parameters that replicated the data. For example, data plotted in the lower left panel shows that when the maximum amplitude of the weakening side of the learning rule is larger than the maximum amplitude of the strengthening side, more parameter sets replicated experimental data.

(H) Plotting the areas of strengthening and weakening (amplitude*τ) of the parameter sets that replicated the data shows that an asymmetric learning rule is needed to replicate experimental data. The filled rectangle indicates all simulated strengthening and weakening area relations.

These simulations predict that the OD bias will shift paradoxically toward the DE, independent of spontaneous EPSC rate in layer 4 (Figure 5D, upper panel dashed line), indicating that subplate neurons are necessary for the normal shift in OD plasticity toward the more active eye. These simulations also show that the strength of the DE will remain close to its initial value, consistent with experimental observations (Kanold et al., 2003). To investigate how spiking activity in subplate neurons might influence thalamocortical plasticity, correlations between LGN spikes, subplate spikes, and cortical spikes were plotted in the model. With subplate neurons present, simulations show that initially, layer 4 spikes follow those of NDE thalamic axons, with an average latency of >5 ms (Figure 5E, T0). This long latency between thalamic and cortical spikes arises because thalamocortical synapses are initially weak and thus unable to induce reliable spiking in layer 4 neurons directly. In contrast, correlations between layer 4 and subplate spikes occur at <5 ms, because subplate neurons trigger spikes in layer 4 via known monosynaptic connections. Thus, the majority of thalamus-driven layer 4 spikes initially arise disynaptically, from LGN to layer 4 via subplate neurons. However, because thalamus-evoked synaptic events fall into the "strengthening" window of the learning rule, their amplitude increases with

development. This rise in synaptic strength shifts correlations between thalamic axons and layer 4 spikes to progressively shorter times, and eventually, LGN inputs drive layer 4 spikes monosynaptically (Figure 5E; T1). In this way the NDE LGN input strengthens sufficiently to provide dominant input to layer 4 (Figure 5B).

Without subplate neurons, simulations show that spikes in LGN axons are no longer correlated with those in layer 4 (Figure 5F). Because NDE LGN axons fire at higher rates than those from the DE, their synaptic events occur more frequently in the "weakening" window of the learning rule; consequently, without the subplate NDE inputs gradually decrease in amplitude. DE LGN synaptic strength is maintained close to its initial state because the DE firing rates are low initially, protecting those synapses from weakening via uncorrelated layer 4 activity. Thus, OD shifts toward the DE in the absence of subplate neurons. These simulations demonstrate two roles for subplate neurons: they can induce strong correlations between thalamic and layer 4 spiking activity, and they can reduce the frequency of cortical EPSCs not correlated with thalamic inputs, establishing conditions favorable for synaptic strengthening.

To test whether the learning rule chosen here is of a general nature, parametric simulations varying amplitudes and time constants of the strengthening and weakening areas of the plasticity rule were performed (Experimental Procedures). Of 4900 different parameter sets, 384 sets achieved a replication of experimental data. Analysis of these 384 parameter sets (Figures 5G and 5H) revealed that only those in which the area under the weakening part of the learning rule is larger than the area under the strengthening part of the learning rule led to a replication of the experimental data. Such asymmetric learning rules are found experimentally in cortex and are predicted by theoretical analyses (Abbott and Nelson, 2000; Bi and Poo, 2001; Dan and Poo, 2004; Feldman, 2000; Froemke and Dan, 2002; Song and Abbott, 2001; Song et al., 2000; Weliky, 2000; Zhou et al., 2003).

Together, these simulations suggest that increased spontaneous EPSC rates by themselves can prevent or even reverse the direction of OD plasticity in layer 4 neurons. Thus, subplate neurons can be viewed as functioning in a circuit that boosts correlations between thalamic and cortical spikes; this in turn leads to strengthening the most frequently active thalamocortical synapses.

Plasticity of OD Columns in Layer 4 Is Paradoxical in Absence of Subplate Neurons

The model prediction of paradoxical OD plasticity was tested experimentally by coupling MD with ablation of subplate neurons just before eye opening in cat (P6–P9), a time when OD columns have not formed yet (Crair et al., 2001) and when inputs from the LGN to layer 4 are weak. The status of OD columns in layer 4 was subsequently assessed at times of normal maturation by injecting transneuronal tracer in either the deprived or nondeprived eye and observing the pattern of labeled thalamocortical axon terminals in layer 4.

As expected, in normal animals LGN axons representing each eye occupy an approximately equal percentage of cortical territory (Figure 6G). Following long-term MD in the presence of subplate neurons, OD columns belonging to the NDE in layer 4 have expanded so dramatically that the pattern of transneuronally transported radioactive label in layer 4 is virtually uniform (Figures 6A and 6C). Correspondingly, the DE OD columns are barely discernable because they have shrunken (Figures 6B and 6C) (Crair et al., 1998; Hubel et al., 1977; Shatz and Stryker, 1978; Wiesel and Hubel, 1963). In contrast, following subplate ablation, the pattern of labeling in layer 4 representing the NDE is patchy rather than uniform (Figure 6D, arrows) indicating that NDE afferents occupy *less* territory in subplate-ablated than in unablated regions (Figures 6D and 6F). At the time of ablation, OD columns have not formed; thus this experiment indicates that NDE LGN axons have lost territory in layer 4. Conversely, in subplate-ablated zones, OD columns representing the DE occupy a *wider* territory than in neighboring unablated regions, indicating that DE LGN axons have retained most of their initial territory (Figures 6E and 6F).

The outcome of OD plasticity in unmanipulated and subplate-ablated animals was quantified by line scans of the autoradiographic signal in layer 4 (Figure S2; Figure 6G). Results indicate that in layer 4 of subplate-ablated cortex, the DE representation is paradoxically *larger* than the NDE representation (Figure 6G). In addition, the sum of DE and NDE representations in ablated areas is larger than that in unablated areas (125% versus 108%), indicating that the representations of the two eyes within layer 4 remain partially overlapping in the absence of subplate neurons (Figure 6F). Thus, while OD column plasticity is still present following subplate ablation, it is altered in the sense that connections driven by the *less* active eye now occupy more territory than those driven by the *more* active eye. Prior experiments have shown that without subplate neurons, even when both eyes are open and LGN neurons relay normal visually driven inputs to cortex, there is no periodic variation of label in layer 4 representing either eye and OD columns fail to form (Ghosh and Shatz, 1992; Kanold et al., 2003). The fundamental difference here is that one eye has now been closed. Together, these experiments confirm the model predictions and reveal an essential requirement for subplate neurons in an activity-based mechanism of OD plasticity following MD.

Discussion

The results of these experiments provide an experimental and a theoretical framework demonstrating that synaptic plasticity during the critical period is the product of a complex and dynamically changing circuit in which subplate neurons play a key role. A strong case linking intact inhibition and OD plasticity has been made from prior studies of development of the visual cortex, based on pharmacological and/or genetic manipulations that perturbed GABAergic function or maturation (reviewed in Hensch, 2004). However, less is known about the specific neurons and circuits that normally function in vivo to drive maturation of inhibition; nor are essential details of the developing thalamocortical circuit well understood. For instance, it is generally assumed that the effects of visual deprivation during the critical period act on an adult-like circuit, but this view is far from accurate, since the subplate neurons

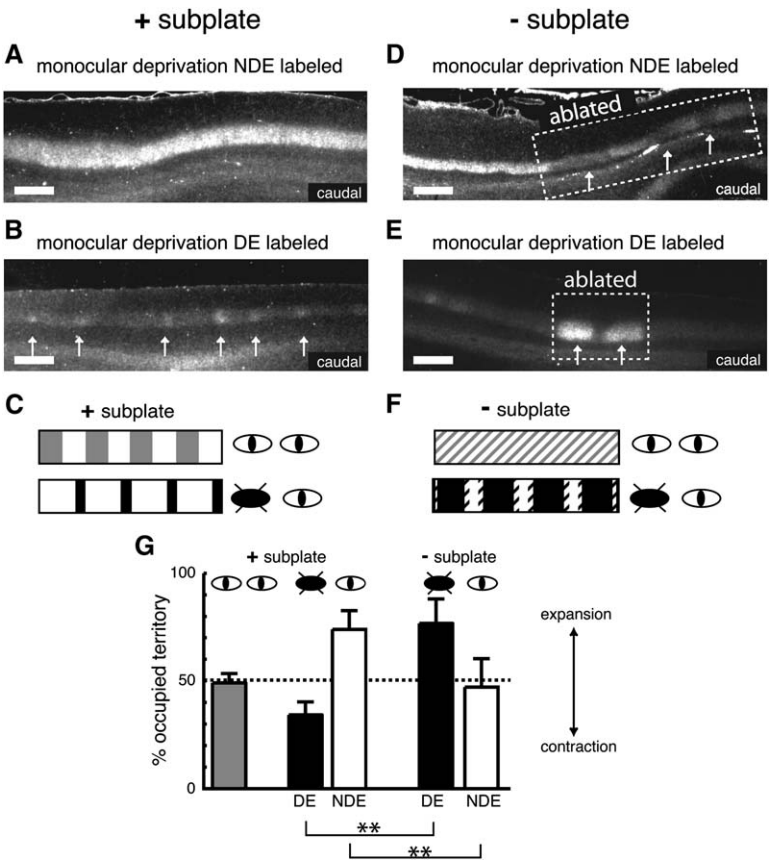

Figure 6. Paradoxical OD Plasticity after Subplate Ablation Combined with Monocular Deprivation

OD columns in layer 4 at 10 weeks after MD beginning at (P6–P7) in animals where the subplate is present ([A] and [B]) or ablated ([D] and [E]). (Upper panels) OD columns in horizontal sections of visual cortex (transneuronal autoradiography). Silver grains, labeling LGN axons and terminals, appear white (see Experimental Procedures). After MD, the NDE columns (A) are wider, while DE columns (B) are faint and narrow (arrows). (C) Schematic summarizing normal OD shift following MD. (D and E) NDE and DE columns at 10 weeks in separate animals receiving subplate ablations plus MD at P6. Scale bars, 1 mm. (D) Labeling of NDE columns in unablated zones is almost continuous, indicating the expected expansion of the NDE after MD. However, in subplate-ablated zones (box), labeling of NDE is weak and patchy. (E) DE columns labeled. Note bright, wide patches in subplate-ablated zone, indicating paradoxical persistence of DE columns (box, arrows), versus faint narrow columns and large inter-column gaps in unablated flanking regions indicating the expected pruning of DE projections after MD. (F) Schematic summarizing the paradoxical OD shift and persistence in overlap of projections from the two eyes in subplate-ablated cortex following MD. (G) Summary histograms (mean + SD) showing relative area (see Experimental Procedures and Figure S2) occupied by thalamic afferents belonging to one eye in normal animals (49% ± 4%, n = 7 sections in n = 3 animals; n = 3 sections from ipsilateral and n = 4 from contralateral cortex) or the DE or NDE in manipulated animals (n = 5 and n = 4 animals, respectively). The % area of DE or NDE following MD are different in ablated versus unablated zones (DE: 77% ± 11% versus 34% ± 6%, n = 16; NDE: 47% ± 13% versus 74% ± 8%, n = 18 sections; both **$p < 0.01$). The percent area was similar in unablated zones in hemisphere receiving ablation and unmanipulated (opposite) hemisphere (DE: n = 23; NDE: n = 9 sections, both $p > 0.1$).

comprise a key component of the developing, but not the adult, thalamocortical circuit. The results of our experiments have identified subplate neurons as essential for the maturation of inhibition and essential for setting the proper direction of OD plasticity within layer 4 following monocular visual deprivation.

Previous studies have shown that in the absence of subplate neurons, excitatory thalamocortical synapses fail to scale up and OD columns do not form (Ghosh and Shatz, 1992; Kanold et al., 2003). These observations suggested to us that LGN inputs representing the two eyes would not be able to remodel at all in the absence of subplate neurons, and we had anticipated that MD under these circumstances would have no effect on OD columns or synaptic plasticity. Thus, it was surprising to find here that eye closure actually causes LGN axons representing the open eye to recede from layer 4, implying that while synaptic strengthening does not occur in the absence of the subplate, synaptic weakening can occur. Our model can help explain why a paradoxical OD shift occurs following MD in the absence of subplate neurons. Computationally, subplate neurons can influence thalamocortical spiking in at least two ways. First, by driving layer 4 neurons to spike when LGN axons spike, subplate neurons correlate activity in the thalamocortical circuit and minimize time periods when the activity of layer 4 neurons is not synchronized with retinally driven activity relayed by LGN axons. Secondly, as shown here, because the subplate is needed to switch cortical GABAergic action from depolarizing to hyperpolarizing, the subplate would also function normally to decrease spontaneous intracortical activity (visible as spontaneous EPSCs in layer 4 neurons), again minimizing cortical spikes uncorrelated with thalamic inputs. This role for the subplate is consistent with experimental observations that mEPSC rates in layer 4 neurons increase after subplate ablation (Kanold et al., 2003). This circuit property of the subplate—to boost correlations between thalamic and cortical spiking patterns—should be considered in any realistic model of how OD plasticity is controlled during the critical period.

Mechanisms of Paradoxical OD Plasticity

In conjunction with prior work, our observations indicate that paradoxical OD plasticity can arise in multiple ways. We show that removing subplate neurons, which effectively decouples cortical activity from thalamic inputs (Kanold et al., 2003), produces paradoxical plasticity that can be understood computationally by an increase in uncorrelated activity between thalamic axons and

layer 4 target neurons. Infusing muscimol (Hata and Stryker, 1994; Hata et al., 1999), APV (Bear et al., 1990; Miller et al., 1989a), or BDNF (Galuske et al., 1996; 2000) into the cortex at later developmental ages in cats can also produce paradoxical OD shifts following MD. All these manipulations alter the visual response properties of cortical neurons and thereby are quite likely to reduce correlations between thalamic and cortical activity. However, there are important differences between the subplate neuron ablations here and the muscimol infusions by Hata et al. (Hata and Stryker, 1994; Hata et al., 1999). The muscimol infusions were performed at 4 weeks postnatal, when thalamic inputs have already scaled up to adult strength and when GABA action is already hyperpolarizing (Figures 1 and 2). While these infusions block spiking, they are unlikely to have affected thalamocortical EPSC rates. Thus, the correlation between the activity of thalamic axons and layer 4 could be severely reduced following muscimol infusion. While OD plasticity in our model depends on postsynaptic spiking responses, if the plasticity rule in layer 4 is modified to produce weakening of thalamic inputs in the absence of postsynaptic firing, for example by an extension of the weakening window to long delays, then our model can also predict the results of Hata et al. (Hata and Stryker, 1994; Hata et al., 1999).

The model also predicts that at a certain value of cortical EPSC frequency increase (or an equivalent decrease in intracortical inhibition), OD plasticity following MD may even be prevented entirely. Indeed, this situation is observed in GAD65 knockout mice, in which cortical neurons lack high-frequency GABAergic inhibition and have elevated discharge rates (prolonged afterdischarges) following visual stimulation (Hensch et al., 1998). While spontaneous *spiking* activity is reported to be within normal ranges (Hensch et al., 1998), it is conceivable that presynaptic spontaneous mEPSC frequency is increased in GAD65 knockout mice, possibly because afferents have not refined so that each layer 4 neuron receives more weak inputs from a variety of thalamocortical and intracortical sources rather than a few strong inputs. The slight increases in spontaneous spiking rate driven by the increased spontaneous EPSC frequency predicted in the model might not be detected physiologically without the use of quantitative microelectrode recordings (Hensch et al., 1998). Indeed, the simulations demonstrate that increased EPSC frequency leads to abnormal OD plasticity without large increases in spiking rates of layer 4 neurons. Thus, the prolonged afterdischarge and increased mEPSC frequency in GAD65 knockout mice could act to reduce periods of correlation at thalamocortical synapses and thereby explain the absence of OD plasticity in these mice.

Contribution of Subplate Neurons to Maturation of Inhibition

The link between ocular dominance plasticity and inhibition was originally noted by Hensch (2004). But how is maturation of inhibitory circuits controlled in vivo? In mice, BDNF overexpression in cortical pyramidal neurons accelerates both maturation of inhibition and the onset and termination of the critical period (Hanover et al., 1999; Huang et al., 1999). However, here we show that subplate ablation prevents maturation of inhibition (Figures 1 and 3), even though BDNF mRNA levels increase after subplate ablation (Lein et al., 1999) (Figure 3D). There are several crucial differences between these studies. First, here we removed a single cell type, and the effects are specific to layer 4, whereas laminar connectivity between layer 4 and 2/3 (Kanold et al., 2003) and inhibition in layer 2/3 appear to develop normally in the absence of the subplate. This selective influence of subplate on layer 4 is likely due to the fact that layer 4 neurons are the principal targets of subplate axons (Friauf et al., 1990; Friauf and Shatz, 1991). The BDNF overexpression experiments in transgenic mice were achieved by driving BDNF to high levels in all pyramidal neurons throughout all cortical layers, whereas the selectivity of subplate ablation alters BDNF via regulatory pathways normally present in cortical neurons. Secondly, the timing of the manipulations is quite different in the two experiments: subplate neurons were ablated in cat well before the onset of the critical period for OD plasticity, whereas BDNF overexpression was timed to ramp up during the critical period in mouse. Clearly, additional experiments confined to layer-restricted cell types and performed at specific ages will be required to reconcile these differences; nonetheless, our experiments indicate that one cell type crucial for maturation of inhibition in cortical layer 4 is the subplate neuron.

Subplate Neurons and Developmental Upregulation of KCC2

GABAergic neurons are abundant in subplate-ablated cortex (Lein et al., 1999), implying that the effect of ablation is read out largely postsynaptically on the layer 4 target neurons receiving GABAergic inputs. How might subplate neurons function normally to regulate maturation of inhibition within cortical layer 4? Subplate neurons are known to provide largely glutamatergic, excitatory inputs to cortex (Finney et al., 1998; Friauf and Shatz, 1991), thereby depolarizing layer 4 cortical neurons even before thalamocortical synapses mature. In hippocampal development, it is thought that sufficient depolarization is needed not only for the strengthening of glutamatergic synapses, but also for the upregulation of KCC2 expression and consequent switch in GABAergic transmission from depolarizing to hyperpolarizing (Ben-Ari, 2002; Ben-Ari et al., 1997; Ganguly et al., 2001; Hennou et al., 2002; Lee et al., 2005; Owens and Kriegstein, 2002; Rivera et al., 1999). In cerebral cortex, without subplate neurons thalamocortical synapses do not scale up in strength and spontaneous activity in cortical circuits is increased (Kanold et al., 2003). In this case, layer 4 neurons might not receive the necessary depolarization for upregulation of KCC2. This view is consistent with our finding that chronically blocking glutamatergic transmission prevents KCC2 upregulation.

Thus, subplate neurons might normally provide excitatory synaptic drive needed for the dual purposes of strengthening excitatory synapses from the thalamus and switching on GABA receptor subunits and KCC2 expression, essential for mature GABAergic inhibition in layer 4. These functions of the subplate might be essential for controlling cortical excitability (Shu et al., 2003) and preventing epilepsy (Mathern et al., 2000;

Jin et al., 2005) during cortical circuit formation. Since subplate neurons are prone to hypoxic injury both in utero and during early postnatal life (McQuillen et al., 2003; Volpe, 1996), it is worth considering the possibility that the dysregulation of inhibition noted in epilepsy and cerebral palsy could arise due to subplate neuron loss.

Experimental Procedures

All experiments were performed according to Harvard Medical School's Institutional Animal Care and Use Committee Protocol. Detailed methods are available in the Supplemental Data.

Surgery and Anesthesia

Ablations

Subplate neurons in visual cortex of 30 cats of both sexes were ablated selectively between P6–P9 by focal injection of either p75-immunotoxin (ME20.4-SAP, Advanced Targeting Systems, 0.5 μl, 0.25–1 mg/ml) or kainic acid (Sigma, 0.5 μl, 10 mg/ml) (control injections: normal saline 0.5 μl) using sterile surgical techniques as described (Ghosh and Shatz, 1992; Kanold et al., 2003; Lein et al., 1999). Fluorescent latex microspheres were added to verify injection sites. At these early ages subplate neuron ablations using either p75-immunotoxin or kainate are highly selective and leave neurons in the overlying cortical plate almost completely intact (Ghosh and Shatz, 1992; Kanold et al., 2003; Lein et al., 1999). At the early ages used in this study (<P40), no atrophy of layer 4 neurons is observed (see Figures 1, 3, 4, and Figure S1) as has been occasionally seen after very long survival times (Ghosh and Shatz, 1994), and electrophysiological and morphological properties of layer 4 neurons in ablated cortex are essentially normal (Kanold et al., 2003). Both ablation methods cause similar anatomical and functional deficits, with p75-immunotoxin injections producing smaller-sized ablations (Kanold et al., 2003). Methods of subplate ablation (p75-immunotoxin, n = 2 animals, versus kainate, n = 3 animals) had similar effects on the DE projections after MD ($p > 0.1$).

Minipump Experiments

Animals (P6–P7) were anesthetized with 3%–4% isofluorane and maintained during surgery at 3%–4%. A craniotomy (~1 mm) was made overlying visual cortex and a canula inserted (~3 mm into cortex) (methods from Bear et al. 1990). The canula was connected to an osmotic minipump (Alzet 2002, 0.5 μl/h) filled with 50 mM DL-AP5 and 10 mM NBQX (disodium salt) in 0.9% sterile saline, specific NMDA and AMPA blockers (Sigma), or 0.9% saline (control). After 1–2 weeks infusion, animals were euthanized with an IP overdose (sodium pentobarbital 200 mg/kg to effect) and brains were rapidly removed. Coronal sections were cut (~1 mm thick) from visual cortex (up to ~2–3 mm from infusion site; in this area a yellow/brown residue is visible, indicating effectiveness of NBQX infusion) and from contralateral visual cortex. RNA was extracted and quantitative PCR for KCC2, $GABA_A$-α1 and HPRT was performed as described below. For each animal, 2–4 samples of the infused and contralateral hemisphere were compared. Since samples from the infused hemisphere likely also included some tissue not receiving effective glutamatergic blockade due to distance from the infusion site, the mRNA levels in the reported average (Figure 3) likely represent an underestimate.

In Situ Hybridizations

Animals received an IP overdose of sodium pentobarbital (200 mg/kg to effect) and the brains were rapidly removed and frozen in cryoprotective medium (M1, Shandon). In-situ hybridizations were performed as described and expression levels were quantified by densitometry (Kanold et al., 2003; Lein et al., 1999).

Slice Physiology

Slices of visual cortex were prepared as described (Kanold et al. 2003). Perforated patch recordings were performed using gramicidin, allowing recording while preserving internal Cl^- concentration. Lucifer yellow (LY) was added to the electrode solution to monitor seal integrity and for post hoc cell identification (see Figure 4D). For recording, slices were held in a chamber and superfused with ACSF containing 100 μM DL-AP5, 10 μM CNQX, and 1 μM TTX. Layer 4 was identified visually by distance from the pial surface (~600–800 μm); location of neurons was confirmed after recording by immunohistochemistry. Muscimol was bath-applied (100 μM) and the evoked current from a holding potential close to the resting potential (~−60 mV) was measured in each cell. The integrity of the patch was monitored and confirmed by fluorescent imaging of Lucifer yellow. Then the patch was ruptured and resulting whole-cell current was measured.

For Ca^{2+} imaging, slices were loaded with Fura 2-AM and superfused with ACSF containing 100 μM DL-AP5 and 10 μM CNQX. In some experiments 0.5–1 μM TTX was added. Muscimol was either bath-applied (50–100 μM in ACSF) or pressure-applied focally (250 μM) with a patch pipette positioned on the surface or up to 50 μm above the slice using a picospritzer (WPI, 4 psi 500 ms–1s). Changes in fluorescence were judged significant if the absolute change (ΔF) exceeded two standard deviations from baseline.

Quantitative PCR

mRNA was obtained from animals receiving an IP overdose of sodium pentobarbital (200 mg/kg to effect). A block of visual cortex from one hemisphere was removed and homogenized in Trizol (Gibco). Total RNA was extracted by chlorophorm and isopropanol precipitation. cDNA was generated from 1 μg RNA by reverse transcription. Real-time PCR reaction was carried out on a Smart Cycler system (Cepheid, Sunnyvale, CA). Glyceraldehyde-3-phosphate dehydrogenase (GAPDH), hypoxanthine phosphoribosyltransferase 1 (HPRT1) and 18S RNA were used as internal normalizing controls. Only 18S remained constant over the observed developmental period; thus all developmental data was normalized to 18S. To compare tissue at the same age, both HPRT1 and 18S were used for normalization.

The number of cycles it took the fluorescence signal to pass an arbitrary threshold of 30 was determined by the Smart Cycler software (typically 18–26 cycles). Difference between the obtained threshold cycle (C_T) for KCC2 (ΔKCC2), $GABA_A$-α1 (Δ$GABA_A$-α1), etc. and the normalizing control were calculated ($\Delta KCC2 = C_{T\ KCC2} - C_{T\ 18S}$ or $\Delta KCC2 = C_{T\ KCC2} - C_{T\ HPRT1}$). For developmental profiles, differences were normalized to the oldest age. Expression levels were calculated from ΔKCC2, Δ$GABA_A$-α1 etc. as 2^(−ΔKCC2) and 2^(−Δ$GABA_A$-α1) respectively.

Transneuronal Labeling

To visualize OD columns under normal circumstances and following MD, 2 mCi of L-[2,3,4,5-^{3}H] proline (Amersham) in 50 μl 0.9% saline was injected into the vitreous chamber of one eye (Ghosh and Shatz, 1992). Darkfield images were analyzed in MATLAB. To quantify the extent of territory belonging to each eye, linescans were made along layer 4 of visual cortex. The fraction of area occupied by radioactive label belonging to the DE in ablated or unablated regions was calculated as $DE_{width}/(DE_{width} + NDE_{width})$, where DE_{width} and NDE_{width} are the sum of all column widths for the respective eye (see Supplemental Data for full details).

Computational Modeling

The subplate neuron and layer 4 neuron were represented by "integrate and fire neurons." If spikes occurred in the layer 4 neuron, the synaptic weights were readjusted according to the plasticity rule (see Figure 5A), giving a plasticity factor Δw(dt) as a function of the delay dt ($dt = t_{spike} - t_{EPSC}$) between the occurrence of the postsynaptic spike and the synaptic input. The parameters of the learning rule were $\tau_S = 3$ ms and $\tau_W = 20$ ms. Parametric simulation of 4900 different parameter sets were performed for four different conditions (+subplate, −subplate, +subplate & MD, −subplate & MD). 384/4900 parameter sets replicated the experimental data. A parameter set was judged as replicating the data when the results in all four conditions fulfilled the following criteria: (1) +subplate: strengthening of thalamic inputs and weakening of subplate input; (2) −subplate: no strengthening of eye1 or eye2 over initial strength; (3) +subplate & MD: strengthening of the open eye and weakening of both subplate inputs and deprived eye; and (4) −subplate & MD: no strengthening of either eye and paradoxical shift.

The model was driven from its initial state by thalamic activity, which was simulated as uncorrelated Poisson processes with spike

rates of 5–10 Hz for the NDE (Dan et al., 1996), and 0.3–1 Hz for the DE. The spontaneous EPSC inputs to the layer 4 neuron was simulated as a 3rd uncorrelated Poisson process with a rate of 0.5 Hz (Kanold et al., 2003) and a weight of 0.7. All data presented was simulated with rates of 5 Hz for the NDE and 0.3 Hz for the DE. Physiologically, OD is frequently measured on a discrete scale where a value of 1 or 7 indicates monocular responses to contralateral or ipsilateral stimulation, respectively. A value of 4 indicates equal responses from the two eyes. An initial bias in OD (estimated mean 3.2) in layer 4 is present at early development (Albus and Wolf, 1984; Hubel and Wiesel, 1963; LeVay et al., 1978), thus slightly favoring the contralateral eye. In the model we measure OD on a finer scale using an OD bias index (OD bias = [Ipsi − Contra]/[Ipsi + Contra]) that varies continuously from −1 to 1. A lack of OD bias is indicated by a value of 0, whereas monocular responses will have values of −1 or +1. The physiologically measured OD values can be translated into OD bias by OD bias = [OD − 4]/3; thus, an OD of 3 is roughly equivalent of an OD bias −0.33. We simulated initial contralateral biases within ($-0.27 \leq$ bias ≤ 0) and outside (bias < -0.27) the physiological range. An initial bias toward the DE or NDE was simulated by reducing the initial weight of one input and by increasing the other to keep total synaptic input constant. To generate correlation plots, a fixed number of layer 4 spikes were selected, and the time differences to spikes of the respective input in a time window of ±50 ms were computed.

Supplemental Data

The Supplemental Data for this article can be found online at http://www.neuron.org/cgi/content/full/51/5/627/DC1/.

Acknowledgments

We thank M. Marcotrigiano, B. Printseva, and Y. Kim for surgical, histological, and technical assistance, and D. Butts, T. GrandPre, M. Majdan and J. Syken for comments on the manuscript. This work was supported by NIH ROI EY02858 (C.J.S.) and F32 EY1352 (P.O.K.).

Received: January 17, 2006
Revised: May 11, 2006
Accepted: July 6, 2006
Published: September 6, 2006

References

Abbott, L.F., and Nelson, S.B. (2000). Synaptic plasticity: taming the beast. Nat. Neurosci. Suppl. *3*, 1178–1183.

Albus, K., and Wolf, W. (1984). Early post-natal development of neuronal function in the kitten's visual cortex: a laminar analysis. J. Physiol. *348*, 153–185.

Allendoerfer, K.L., and Shatz, C.J. (1994). The subplate, a transient neocortical structure: its role in the development of connections between thalamus and cortex. Annu. Rev. Neurosci. *17*, 185–218.

Baumfalk, U., and Albus, K. (1987). Baclofen inhibits the spontaneous and visually evoked responses of neurones in the striate cortex of the cat. Neurosci. Lett. *75*, 187–192.

Bear, M.F., Kleinschmidt, A., Gu, Q.A., and Singer, W. (1990). Disruption of experience-dependent synaptic modifications in striate cortex by infusion of an NMDA receptor antagonist. J. Neurosci. *10*, 909–925.

Ben-Ari, Y. (2002). Excitatory actions of gaba during development: the nature of the nurture. Nat. Rev. Neurosci. *3*, 728–739.

Ben-Ari, Y., Khazipov, R., Leinekugel, X., Caillard, O., and Gaiarsa, J.L. (1997). GABAA, NMDA and AMPA receptors: a developmentally regulated 'menage a trois'. Trends Neurosci. *20*, 523–529.

Bi, G., and Poo, M. (2001). Synaptic modification by correlated activity: Hebb's postulate revisited. Annu. Rev. Neurosci. *24*, 139–166.

Chen, L., Yang, C., and Mower, G.D. (2001). Developmental changes in the expression of GABA(A) receptor subunits (alpha(1), alpha(2), alpha(3)) in the cat visual cortex and the effects of dark rearing. Brain Res. Mol. Brain Res. *88*, 135–143.

Crair, M.C., Gillespie, D.C., and Stryker, M.P. (1998). The role of visual experience in the development of columns in cat visual cortex. Science *279*, 566–570.

Crair, M.C., Horton, J.C., Antonini, A., and Stryker, M.P. (2001). Emergence of ocular dominance columns in cat visual cortex by 2 weeks of age. J. Comp. Neurol. *430*, 235–249.

Dan, Y., and Poo, M.M. (2004). Spike timing-dependent plasticity of neural circuits. Neuron *44*, 23–30.

Dan, Y., Atick, J.J., and Reid, R.C. (1996). Efficient coding of natural scenes in the lateral geniculate nucleus: experimental test of a computational theory. J. Neurosci. *16*, 3351–3362.

Douglas, R.J., and Martin, K.A. (2004). Neuronal circuits of the neocortex. Annu. Rev. Neurosci. *27*, 419–451.

Fagiolini, M., and Hensch, T.K. (2000). Inhibitory threshold for critical-period activation in primary visual cortex. Nature *404*, 183–186.

Feldman, D.E. (2000). Timing-based LTP and LTD at vertical inputs to layer II/III pyramidal cells in rat barrel cortex. Neuron *27*, 45–56.

Finney, E.M., Stone, J.R., and Shatz, C.J. (1998). Major glutamatergic projection from subplate into visual cortex during development. J. Comp. Neurol. *398*, 105–118.

Friauf, E., and Shatz, C.J. (1991). Changing patterns of synaptic input to subplate and cortical plate during development of visual cortex. J. Neurophysiol. *66*, 2059–2071.

Friauf, E., McConnell, S.K., and Shatz, C.J. (1990). Functional synaptic circuits in the subplate during fetal and early postnatal development of cat visual cortex. J. Neurosci. *10*, 2601–2613.

Froemke, R.C., and Dan, Y. (2002). Spike-timing-dependent synaptic modification induced by natural spike trains. Nature *416*, 433–438.

Galuske, R.A., Kim, D.S., Castren, E., Thoenen, H., and Singer, W. (1996). Brain-derived neurotrophic factor reversed experience-dependent synaptic modifications in kitten visual cortex. Eur. J. Neurosci. *8*, 1554–1559.

Galuske, R.A., Kim, D.S., Castren, E., and Singer, W. (2000). Differential effects of neurotrophins on ocular dominance plasticity in developing and adult cat visual cortex. Eur. J. Neurosci. *12*, 3315–3330.

Ganguly, K., Schinder, A.F., Wong, S.T., and Poo, M. (2001). GABA itself promotes the developmental switch of neuronal GABAergic responses from excitation to inhibition. Cell *105*, 521–532.

Ghosh, A., and Shatz, C.J. (1992). Involvement of subplate neurons in the formation of ocular dominance columns. Science *255*, 1441–1443.

Ghosh, A., and Shatz, C.J. (1994). Segregation of geniculocortical afferents during the critical period: a role for subplate neurons. J. Neurosci. *14*, 3862–3880.

Ghosh, A., Antonini, A., McConnell, S.K., and Shatz, C.J. (1990). Requirement for subplate neurons in the formation of thalamocortical connections. Nature *347*, 179–181.

Golshani, P., Truong, H., and Jones, E.G. (1997). Developmental expression of GABA(A) receptor subunit and GAD genes in mouse somatosensory barrel cortex. J. Comp. Neurol. *383*, 199–219.

Hanover, J.L., Huang, Z.J., Tonegawa, S., and Stryker, M.P. (1999). Brain-derived neurotrophic factor overexpression induces precocious critical period in mouse visual cortex. J. Neurosci. *19*, RC40.

Hata, Y., and Stryker, M.P. (1994). Control of thalamocortical afferent rearrangement by postsynaptic activity in developing visual cortex. Science *265*, 1732–1735.

Hata, Y., Tsumoto, T., and Stryker, M.P. (1999). Selective pruning of more active afferents when cat visual cortex is pharmacologically inhibited. Neuron *22*, 375–381.

Hennou, S., Khalilov, I., Diabira, D., Ben-Ari, Y., and Gozlan, H. (2002). Early sequential formation of functional GABAA and glutamatergic synapses on CA1 interneurons of the rat foetal hippocampus. Eur. J. Neurosci. *16*, 197–208.

Hensch, T.K. (2004). Critical period regulation. Annu. Rev. Neurosci. *27*, 549–579.

Hensch, T.K., Fagiolini, M., Mataga, N., Stryker, M.P., Baekkeskov, S., and Kash, S.F. (1998). Local GABA circuit control of experience-

dependent plasticity in developing visual cortex. Science *282*, 1504–1508.

Herrmann, K., Antonini, A., and Shatz, C.J. (1994). Ultrastructural evidence for synaptic interactions between thalamocortical axons and subplate neurons. Eur. J. Neurosci. *6*, 1729–1742.

Huang, Z.J., Kirkwood, A., Pizzorusso, T., Porciatti, V., Morales, B., Bear, M.F., Maffei, L., and Tonegawa, S. (1999). BDNF regulates the maturation of inhibition and the critical period of plasticity in mouse visual cortex. Cell *98*, 739–755.

Hubel, D.H., and Wiesel, T.N. (1963). Receptive fields of cells in striate cortex of very young, visually inexperienced kittens. J. Neurophysiol. *26*, 994–1002.

Hubel, D.H., Wiesel, T.N., and LeVay, S. (1977). Plasticity of ocular dominance columns in monkey striate cortex. Philos. Trans. R. Soc. Lond. B Biol. Sci. *278*, 377–409.

Hubner, C.A., Stein, V., Hermans-Borgmeyer, I., Meyer, T., Ballanyi, K., and Jentsch, T.J. (2001). Disruption of KCC2 reveals an essential role of K-Cl cotransport already in early synaptic inhibition. Neuron *30*, 515–524.

Huntsman, M.M., Munoz, A., and Jones, E.G. (1999). Temporal modulation of GABA(A) receptor subunit gene expression in developing monkey cerebral cortex. Neuroscience *91*, 1223–1245.

Jin, X., Huguenard, J.R., and Prince, D.A. (2005). Impaired Cl- extrusion in layer V pyramidal neurons of chronically injured epileptogenic neocortex. J. Neurophysiol. *93*, 2117–2126.

Kanold, P.O., Kara, P., Reid, R.C., and Shatz, C.J. (2003). Role of subplate neurons in functional maturation of visual cortical columns. Science *301*, 521–525.

Lee, H., Chen, C.X., Liu, Y.J., Aizenman, E., and Kandler, K. (2005). KCC2 expression in immature rat cortical neurons is sufficient to switch the polarity of GABA responses. Eur. J. Neurosci. *21*, 2593–2599.

Lein, E.S., Finney, E.M., McQuillen, P.S., and Shatz, C.J. (1999). Subplate neuron ablation alters neurotrophin expression and ocular dominance column formation. Proc. Natl. Acad. Sci. USA *96*, 13491–13495.

LeVay, S., Stryker, M.P., and Shatz, C.J. (1978). Ocular dominance columns and their development in layer IV of the cat's visual cortex: a quantitative study. J. Comp. Neurol. *179*, 223–244.

Lu, J., Karadsheh, M., and Delpire, E. (1999). Developmental regulation of the neuronal-specific isoform of K-Cl cotransporter KCC2 in postnatal rat brains. J. Neurobiol. *39*, 558–568.

Mathern, G.W., Cepeda, C., Hurst, R.S., Flores-Hernandez, J., Mendoza, D., and Levine, M.S. (2000). Neurons recorded from pediatric epilepsy surgery patients with cortical dysplasia. Epilepsia *41*, S162–S167.

McQuillen, P.S., Sheldon, R.A., Shatz, C.J., and Ferriero, D.M. (2003). Selective vulnerability of subplate neurons after early neonatal hypoxia-ischemia. J. Neurosci. *23*, 3308–3315.

Miller, K.D., Chapman, B., and Stryker, M.P. (1989a). Visual responses in adult cat visual cortex depend on N-methyl-D-aspartate receptors. Proc. Natl. Acad. Sci. USA *86*, 5183–5187.

Miller, K.D., Keller, J.B., and Stryker, M.P. (1989b). Ocular dominance column development: analysis and simulation. Science *245*, 605–615.

Owens, D.F., and Kriegstein, A.R. (2002). Is there more to GABA than synaptic inhibition? Nat. Rev. Neurosci. *3*, 715–727.

Owens, D.F., Boyce, L.H., Davis, M.B., and Kriegstein, A.R. (1996). Excitatory GABA responses in embryonic and neonatal cortical slices demonstrated by gramicidin perforated-patch recordings and calcium imaging. J. Neurosci. *16*, 6414–6423.

Rivera, C., Voipio, J., Payne, J.A., Ruusuvuori, E., Lahtinen, H., Lamsa, K., Pirvola, U., Saarma, M., and Kaila, K. (1999). The K+/Cl- co-transporter KCC2 renders GABA hyperpolarizing during neuronal maturation. Nature *397*, 251–255.

Shatz, C.J., and Stryker, M.P. (1978). Ocular dominance in layer IV of the cat's visual cortex and the effects of monocular deprivation. J. Physiol. *281*, 267–283.

Shu, Y., Hasenstaub, A., and McCormick, D.A. (2003). Turning on and off recurrent balanced cortical activity. Nature *423*, 288–293.

Song, S., and Abbott, L.F. (2001). Cortical development and remapping through spike timing-dependent plasticity. Neuron *32*, 339–350.

Song, S., Miller, K.D., and Abbott, L.F. (2000). Competitive Hebbian learning through spike-timing-dependent synaptic plasticity. Nat. Neurosci. *3*, 919–926.

Volpe, J.J. (1996). Subplate neurons–missing link in brain injury of the premature infant? Pediatrics *97*, 112–113.

Weliky, M. (2000). Correlated neuronal activity and visual cortical development. Neuron *27*, 427–430.

Wiesel, T.N., and Hubel, D.H. (1963). Single-cell responses in striate cortex of kittens deprived of vision in one eye. J. Neurophysiol. *26*, 1003–1017.

Yao, H., and Dan, Y. (2001). Stimulus timing-dependent plasticity in cortical processing of orientation. Neuron *32*, 315–323.

Zhou, Q., Tao, H.W., and Poo, M.M. (2003). Reversal and stabilization of synaptic modifications in a developing visual system. Science *300*, 1953–1957.